quinolin-12(13*H*)-one (3). To a solution of naltrexone hydrochloride (2 g, 5.3 mmol) and 1 N NaOH (20 mL, 20 mmol) in MeOH (40 mL) was added methyl vinyl ketone (1 mL, 12.3 mmol) in an ice bath. After the mixture was stirred at room temperature for 14 h under nitrogen, additional methyl vinyl ketone (0.3 mL, 3.7 mmol) was added. The mixture was stirred for 2 h and then neutralized with 10% HCl and 1 N HCl. The resulting mixture was concentrated and extracted with $CHCl_3$ (3×). The combined chloroform extracts were washed with brine and dried, and the solvent was removed to give a crude product, which was purified on a Sephadex column (LH-20, MeOH) to afford a solid, which was recrystallized from AcOEt to yield pure **3** (1.68 g, 80%), mp 252–254 °C: IR (KBr, cm^{-1}) 3400 (OH), 1718 (ketone); ^1H NMR ($CDCl_3$) (see Table I); MS (EI), *m/e* 411 (M^+). Anal. Calcd for $C_{24}H_{29}O_5N$: C, 70.07; H, 7.06; N, 3.41. Found: C, 69.88; H, 7.22; N, 3.45.

[8*R*-(4b*R,8α,8aβ,9aβ,13bβ)]-7-(Cyclopropylmethyl)-6,7,8,8a,9,9a,10,11-octahydro-1,8a-dihydroxy-4,8-methano-5*H*-benzo[*g*]benzofuro[3,2-*e*]isoquinolin-12(13b*H*)-one (4).** A solution of **3** (210 mg, 0.51 mmol) in a mixture of 1 N HCl (2 mL) and MeOH (3 mL) was allowed to stand at 23 °C for 9 days. The solution was neutralized with 1 N NaOH, concentrated, and extracted with $CHCl_3$ (3×). The combined chloroform extracts were washed with brine and dried, and the solvent was removed to give a crude product, which was recrystallized from $CHCl_3$ to afford the α,β-unsaturated ketone **4** (130 mg, 65%), mp 230 °C dec: IR (KBr, cm^{-1}) 3400 (OH), 1675 (conjugated ketone), 1616 (double bond); ^1H NMR ($CDCl_3$) δ 5.05 (s, 1 H, 5-H), 6.50 (d, 1 H, *J* = 2.4 Hz, 21-H vinyl); MS (FAB) 393 (M^+). Anal. Calcd for $C_{24}H_{27}O_4N \cdot 0.2CHCl_3 \cdot 2.4H_2O$: C, 62.60; H, 6.43; N, 3.04. Found: C, 62.60; H, 6.74; N, 3.20.

[8*R*-(4b*R,8α,8aβ,13bβ)]-7-(Cyclopropylmethyl)-6,7,8,8a,9,10,11,13b-octahydro-1,8a-dihydroxy-4,8-methano-5*H*-benzo[*g*]benzofuro[3,2-*e*]isoquinolin-12(13*H*)-one (5).** A solution of **4** (135 mg, 0.30 mmol) in a mixture of AcOH (6 mL) and water (3 mL) was stirred under reflux for 48 h. After concentration of the solution, $CHCl_3$ was added and the mixture was neutralized with saturated $NaHCO_3$ and separated. The aqueous phase was extracted with $CHCl_3$ (3×). The combined organic phases were washed with brine and dried, and the solvent was removed to give a crude product. The product was purified by preparative TLC (silica gel, 7% MeOH in saturated NH_4OH–$CHCl_3$) to afford pure unconjugated ketone **5** (90 mg, 70%): IR (KBr, cm^{-1}) 3400 (OH), 1700 (unconjugated ketone); high-resolution MS (EI), *m/e* 393.1945 (calcd for $C_{24}H_{27}O_4N$ 393.1952).

Acknowledgment. This work was supported by the National Institute on Drug Abuse.

Photocycloaddition of 4,5′,8-Trimethylpsoralen and Oleic Acid Methyl Ester: Product Structures and Reaction Mechanism†

Kathleen G. Specht,‡,∥ W. Robert Midden,*,§ and Miles R. Chedekel‡,⊥

The Center for Photochemical Sciences, Department of Chemistry, Bowling Green State University, Bowling Green, Ohio 43403, and Division of Environmental Chemistry, School of Hygiene and Public Health, The Johns Hopkins University, Baltimore, Maryland 21205

Received February 14, 1989

The stereochemical structures of the four adducts formed between oleic acid methyl ester (OAME) and 4,5′,8-trimethylpsoralen (tmPso) have been determined. Assignment of the tmPso ^1H NMR spectrum was accomplished by analogy to two coumarin model compounds and with the use of homonuclear decoupling and resonance enhancement. Assignment of the ^1H NMR spectra for the OAME–tmPso adducts was made by analogy to the spectra of OAME and tmPso and using 2D *J*-resolved and COSY analyses. The configurations of the cyclobutyl rings in these adducts was determined by MM2 energy minimization calculations, homonuclear ^1H NOE analysis, and comparison of products obtained with *cis*-OAME and *trans*-EAME (elaidic acid methyl ester). Only four of the eight possible disastereomeric adducts are detected. These adducts have the cis-cis-HH, cis-cis-HT, trans-cis-HH, and trans-cis-HT configurations. The lack of formation of the other isomers may be due to the geometric requirements of exciplex formation. The mechanism of the reaction was established to involve initial bond formation at the 4 position of tmPso, most likely to form a diradical intermediate. The rate of dissociation of the trans diradical is much faster than ring closure, in contrast to the cis diradical whose rate of ring closure is at least as fast as dissociation. The rate of cis–trans isomerization of the 9,10-bond of the fatty ester portion of the diradical is faster than ring closure for the cis diradical and slower than ring closure for the trans diradical.

Introduction

Psoralens, the linear members of the furocoumarin family, are some of the most effective agents available for the photochemotherapy of a number of skin diseases such as psoriasis and vitiligo.[1] The therapeutic benefit of this treatment is thought to be due to the inhibition of hyperproliferation of the skin keratinocytes. The use of psoralens is limited due to their carcinogenicity.[2] The chemical mechanisms of psoralens have been studied for almost 20 years with the hope that a way could be found to eliminate psoralen carcinogenicity while retaining the beneficial antiproliferative effect.

Psoralens photochemically add to the 5,6-bond of pyrimidines in DNA, forming cyclobutyl-linked adducts.[3-7]

* To whom correspondence should be addressed.
‡ The John Hopkins University.
§ Bowling Green State University.
∥ Current address: Center for Photochemical Sciences, Department of Chemistry, Bowling Green State University, Bowling Green, OH 43403.
⊥ Current address: Advanced Polymer Systems, 3696 Haven St., Redwood City, CA 94063.

† Abbreviations. OAME: *cis*-oleic acid methyl ester. EAME: *trans*-elaidic acid methyl ester. tmPso: 4,5′,8-trimethylpsoralen. 8-MOP: 8-methoxypsoralen. DMC: 4,8-dimethyl-7-methoxycoumarin. DAC: 4,8-dimethyl-7-acetoxycoumarin. PUVA: psoralen plus UVA.

(1) Fitzpatrick, T. B.; Pathak, M. A. *National Cancer Institute Monograph 66*, **1984**, 3–11.
(2) Roelandts, R. *Arch. Dermatol.* **1984**, *120*, 662–669.
(3) Song, P. S.; Tapley, K. J., Jr. *Photochem. Photobiol.* **1979**, *29*, 1177–1197.
(4) Parsons, B. J. *Photochem. Photobiol.* **1980**, *32*, 813–821.

0022-3263/89/1954-4125$01.50/0

The carcinogenicity of psoralens is very likely due to this reaction.[3,4] It has been proposed that psoralen–DNA adducts are also responsible for the therapeutic antiproliferative effect of psoralens, since no other reactions could be found that might cause such an effect.[8] However, recently we have proven that psoralens also form covalent adducts with unsaturated fatty acids[9,10] and other evidence suggests that such adducts could account for the antiproliferative effect of psoralens by inhibiting a key cell regulatory pathway involving phospholipase C and protein kinase C.[11-16] If this is true, then it should be possible to design safer psoralens that lack the ability to bind to DNA and the associated carcinogenicity while retaining the ability to bind to lipids and the associated therapeutic benefit. Further investigations of the biochemistry of psoralens are needed to evaluate this hypothesis and these investigations would benefit from knowledge of the chemical structures of representative psoralen–lipid adducts.

We have now established the stereochemical structures of four covalent adducts that are formed between one of the most studied psoralens, tmPso (4,5′,8-trimethylpsoralen), and OAME (oleic acid methyl ester), a monounsaturated fatty acid found in abundance in lipids of many living organisms. These are the first structures to be established for covalent psoralen–fatty acid adducts. The structures were determined by ^{1}H NMR spectroscopy using homonuclear decoupling, two-dimensional COSY and J-resolved analyses, and nuclear Overhauser effect experiments and by analysis of reactions of the trans analogue of OAME, elaidic acid methyl ester (EAME). The relative rates of some of the intermediate steps in the reaction were determined by analyses of product yields. The IR absorbance spectra of the adducts are reported as an aid in characterization of these compounds. The solvent dependence of adduct formation was measured to determine the possibility of adduct formation in relatively nonpolar lipid environments.

Results

Isolation and Purification of the tmPso–OAME Photoproducts. Four compounds were isolated by preparative HPLC from a mixture of tmPso and a 5-fold molar excess of OAME, illuminated with 360-nm UV light in ethanol. A fifth photoproduct has been identified as EAME (elaidic acid methyl ester), the trans isomer of OAME. The quantum yield for the sum of the four photoadducts was found to be 0.003. The only other fatty acid product detected is the trans isomer, EAME, formed with a quantum yield of 0.012. The other products detected were products of tmPso photolysis, which occur even in the absence of OAME.

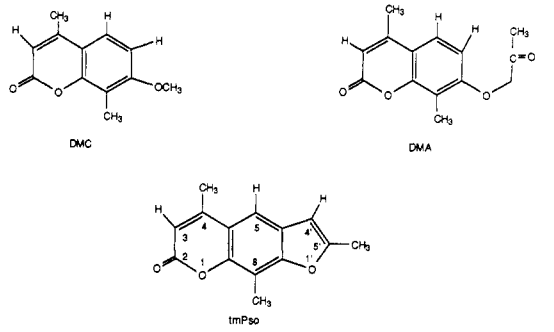

Figure 1. Structures of coumarin model compounds and 4,5′,8-trimethylpsoralen.

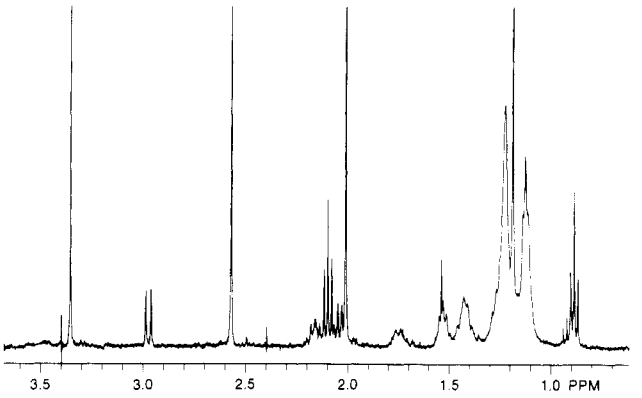

Figure 2. NMR spectrum (400 MHz) of photoadduct 1 from 0 to 3.5 ppm in benzene-d_6. NMR spectrum of photoadduct 3 was nearly identical with this.

The empirical formula is the same for all four of the tmPso–OAME adducts, $C_{32}H_{48}O_5$, as established from their exact masses, 524.3512, 524.3510, 524.3510, and 524.3499, determined by high-resolution mass spectrometry, which are in good agreement with the calculated value of 524.3502. Analysis of the ^{1}H NMR spectra of these compounds required assignment of the spectrum for tmPso since this has not been previously published.

^{1}H NMR Assignments of tmPso in Benzene-d_6. Two substituted coumarins, 4,8-dimethyl-7-methoxycoumarin (DMC) and 4,8-dimethyl-7-acetoxycoumarin (DMA), were used as model compounds to aid the assignment of the ^{1}H NMR spectrum of tmPso (Figure 1). Resonance enhancement and homonuclear decoupling were used to assign the proton spectra of the coumarins. Comparison of the tmPso NMR results with the NMR analysis of the coumarins enabled unambiguous assignments of the tmPso signals: 7.00 ppm = H-5, 6.08 ppm = H-4′, 5.90 ppm = H-3, 2.59 ppm = CH_3-8, 2.00 ppm = CH_3-5′, 1.71 ppm = CH_3-4. Decoupling results and assignments for the coumarins are available in the supplementary material.

^{1}H NMR Analysis of Adducts 1 and 3. The four photoadducts had retention volumes of 19.5, 20.5, 23.0, and 25.0 mL, numbered 1–4 according to their order of elution from a 4.6 × 250 mm Alltech 5-μm C18 column at 2 mL/min with CH_3CN/H_2O, 90:10 (v/v). The ratio of their yields was 5:1:5:1. Their UV absorbance spectra, determined with a diode array spectrophotometric HPLC detector, do not significantly differ. Details of the chromatographic properties and UV absorbance spectra of the four OAME–tmPso photoproducts have been described previously.[9]

(5) Straub, K.; Kanne, D.; Hearst, J. E.; Rapoport, H. *J. Am. Chem. Soc.* **1981**, *103*, 2347–2355.
(6) Kanne, D.; Straub, K.; Hearst, J. E.; Rapoport, H. *J. Am. Chem. Soc.* **1982**, *104*, 6754–6764.
(7) Kanne, D.; Straub, K.; Rapoport, H.; Hearst, J. E. *Biochemistry* **1982**, *21*, 861–71.
(8) Grekin, D. A.; Epstein, J. H. *Photochem. Photobiol.* **1981**, *33*, 957–960.
(9) Specht, K. G.; Kittler, L.; Midden, W. R. *Photochem. Photobiol.* **1988**, *47*, 537–541.
(10) Specht, K. G.; Bhan, P.; Chedekel, M. R.; Midden, W. R. *NATO ASI Series*; Moreno, G., Pottier, R. H., Truscott, T. G., Eds.; Springer-Verlag: Heidelberg, 1987; Vol. 15, pp 301–303.
(11) Laskin, J. D.; Lee, E.; Yurkow, E. J.; Laskin, D. L.; Gallo, M. A. *Proc. Nat. Acad. Sci. U.S.A.* **1982**, *82*, 6158–6162.
(12) Wennersten, G. *Acta. Dermatol. Venereol. (Stockholm)* **1979**, *59*, 21–26.
(13) Meffert, H.; Bohm, F.; Bauer, E. *Stud. Biophys.* **1983**, *94*, 41–44.
(14) Fisher, G. J.; Kragballe, K.; Voorhees, J. J. *Psoriasis, Proceedings of the Fourth International Symposium*; Farber, E. M., Nall, L., Morhenn, V., Jacobs, P. H., Eds.; Elsevier Science Publishing Co., Inc.; New York, 1987; pp 255–261.
(15) Laskin, J. D.; Lee, E.; Laskin, D. L.; Gallo, M. A. *Proc. Natl. Acad. Sci. U.S.A.* **1986**, *83*, 8211–8215.
(16) Midden, W. R. *Psoralen DNA Photobiology*; Gasparro, F. P., Ed.; CRC Press, Inc.: Boca Raton, FL, 1988; Vol. II, pp 1–49.

Table I. Results of 400-MHz Decoupling Experiments for Adducts 1 and 3 in Benzene-d_6

chemical shift (ppm)				
adduct 1	adduct 3	mult (integrtn)	coupled[a] to	assignment[b]
7.20	7.20			solvent benzene (residual ^{1}H)
7.00	7.00	s (1)		[tmPso H-5]
6.08	6.08	s (1)		[tmPso H-4']
3.35	3.35	s (3)		[OAME OCH_3]
2.96	2.96	d (1)	2.16 (m to q)	cyclobutyl H-a [tmPso H-3]
2.59	2.59	s (3)		[tmPso CH_3-8]
2.16	2.16	m (1)	2.96 (d to s) 2.03 (m to q)	cyclobutyl H-b [OAME H-9 or 10]
2.07	2.07	t (2)		[OAME CH_2-2, α to ester C=O]
2.03	2.03	m (1)	2.16 (m to q)	cyclobutyl H-c [OAME H-9 or 10]
2.00	2.00	s (3)		[tmPso CH_3-5']
1.71	1.71	q (2)	2.16 (m to q)	cyclobutyl CH_2-b [OAME CH_2-8 or 11]
1.55	1.50	m		[OAME $(CH_2)_n$]
1.42	1.38	m		[OAME $(CH_2)_n$]
1.19	1.19	s (3)		cyclobutyl CH_3-d [tmPso CH_3-4]
1.30–1.08	1.30–1.08	m (overlapping)		[OAME $(CH_2)_n$]
0.97	0.97	t (3)		[OAME 18-CH_3]

[a] Irradiating the signal in the chemical shift column altered the structure of the signal listed in this column. Text in parentheses indicates the change in signal shape observed upon decoupling. Abbreviations: s = singlet, d = doublet, t = triplet, q = quartet. [b] The positions on the cyclobutyl ring are labeled a, b, c, and d as indicated in Figure 3. The text in brackets indicates the protons in the reactant from which these protons in the product are derived.

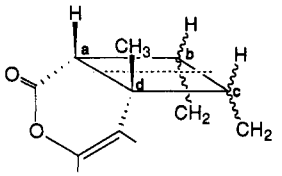

Figure 3. Labeling of the cyclobutyl ring for the four photoadducts.

The upfield portion of the 400-MHz ^{1}H NMR spectrum of photoadduct 1 is illustrated in Figure 2. The NMR spectra of photoadducts 1 and 3, the two photoadducts formed in highest yield, are essentially identical, each having ^{1}H NMR signals characteristic of both the tmPso and OAME starting materials, as well as signals corresponding to those of a cyclobutane adduct. In the ^{1}H NMR spectra of the parent OAME, most of the protons resonate upfield, with the exception of the signals of the two protons on the 9,10-double bond of OAME at 5.5 ppm, the ester OCH_3 at 3.40 ppm, and the CH_2 at 2.07 ppm, which is α to the ester carbonyl. The parent tmPso proton signals were described above.

In the ^{1}H NMR spectra of photoadducts 1 and 3, the resonances of the OAME double bond protons, as well as the signals of the tmPso 3-H and 4-CH_3 group, have shifted upfield with respect to the same proton resonances in the parent compounds. The 4-CH_3 group resonates at 1.19 ppm in the photoadducts and three new signals are detected as a doublet at 2.96 ppm, a multiplet at 2.16 ppm, and a quartet, which is partially buried under the other signals, at 2.03 ppm. Each of the last three signals integrates as one proton. The positions of the cyclobutyl ring in the photoadducts are designated by letters a–d as indicated in Figure 3.

Homonuclear spin decoupling and 2D COSY experiments were used to make the chemical shift assignments. The results of the homonuclear spin decoupling experiments of adducts 1 and 3 are identical. Two-dimensional COSY (COrrelated SpectroscopY) spectra of photoadduct 1 were also obtained (data not shown) to confirm the one-dimensional decoupling results. COSY is especially useful for selectively decoupling a single proton in an area of overlapping proton resonances. These results, as well as the chemical shift assignments, are summarized in Table I.

Analysis of the decoupling and COSY results for photoadducts 1 and 3 indicate that the doublet at 2.96 ppm can be assigned as H-a on the cyclobutyl ring, originating from position-3 on the furocoumarin moiety. H-a is coupled to the proton at 2.16 ppm. This proton at 2.16 ppm is assigned as the adjacent cyclobutyl proton at position-b, which is derived from the 9 or 10 position of the OAME double bond. It is coupled to H-a and CH_2-b and is therefore split into a multiplet. H-b is also coupled to the signal at 2.03 ppm, which is therefore assigned as the third cyclobutyl proton, c, originating from either the 9 or 10 position on OAME. H-c is coupled to H-b and one methylene group, giving a splitting pattern of a quartet. Irradiation of the multiplet at 1.71 ppm decouples the H-b resonance at 2.16 ppm. This multiplet at 1.71 ppm integrates as two protons and is assigned as the methylene group attached to position b on the cyclobutyl ring (CH_2-b). The other cyclobutyl methylene group at the c position of the cyclobutyl ring is not resolved from the other fatty acid protons. These NMR results confirm the formation of cyclobutane adducts involving the 3,4-bond of the furocoumarin and the 9,10-double bond of OAME.

The stereochemical configuration around the cyclobutyl ring of photoadducts 1 and 3 was determined by 500-MHz ^{1}H NOE experiments. Assignment of the stereochemical configuration of the isolated photoadducts was made by assuming that the cyclobutane ring is nearly planar or only slightly puckered and therefore only those ring substituents that are on the same side of the ring (cis) will be close enough to exhibit an NOE interaction. The validity of this assumption was checked by MM2 energy minimization calculations of the ring pucker and dihedral angles of the cyclobutyl substituents in selected model compounds.[17]

The model compounds for MM2 calculations were constructed to include the cyclobutane ring and the substituents that would exert significant effects on the conformation of the cyclobutane ring in each of four possible configurations. These configurations varied in the position of the lactone ring (representing the furocoumarin ring) relative to the methyl groups (representing the fatty acid chains) at positions b and c of the cyclobutyl ring: methyls

(17) Biurkert, U.; Allinger, N. L. *Molecular Mechanics*; ACS Monograph 177; American Chemical Society: Washington, DC, 1982. Allinger, N. L.; et al. *QCPE* **1981**, *13*, 395.

Table II. Results of Energy Minimization Calculations for Models of the Cyclobutyl Adducts of tmPso and OAME

configrtn	angle, deg: ring pucker[a]	angle, deg: dihedral[b]
cis/exo	0.3	2.6
cis/endo	12.1	13.7
trans A	18.0	24.9
trans B	18.2	28.0

[a] The mean of the dihedral angles for the C–C–C bonds around the cyclobutyl ring. [b] The mean of the two dihedral angles for cis vicinal substituents at the b and c positions of the cyclobutyl ring.

Table III. Results of 500-MHz Homonuclear ^{1}H NOE Experiments for Photoadducts 1 and 3 in Benzene-d_6

irradiated	adduct 1: %NOE	adduct 1: ppm[a]	adduct 3: %NOE	adduct 3: ppm
2.96 ppm cyclobutyl H-a	8.15 2.63 *b*	2.16 H-b 1.19 CH_3-d 2.03 H-c	7.21 4.23 *b*	2.16 H-b 1.19 CH_3-d 2.03 H-c
2.16 ppm cyclobutyl H-b	9.62 1.84	2.96 H-a 1.19 CH_3-d	11.84 2.73	2.96 H-a 1.19 CH_3-d
2.03 ppm cyclobutyl H-c	2.37 1.21 0.89	7.01 [H-5 tmPso] 2.96 H-a 1.19 CH_3-d		N.D.[d]
1.71 ppm cyclobutyl CH_2-b		N.D.[d]	34.87	1.38 [$(CH_2)_n$][e]
1.19 ppm cyclobutyl CH_3-d	11.02 8.22 4.51	7.01 [H-5 tmPso] 2.96 H-a 2.16 H-b	12.96 10.30 5.97	[H-5 tmPso] 2.96 H-a 2.16 H-b

[a] The positions on the cyclobutyl ring are labeled a, b, c, and d as indicated in Figure 3. [b] Uncertain due to overlapping signals, possibly a weak enhancement. [c] Weak enhancement, uncertain due to nearness of irradiated signal. When the 2.03 ppm signal was irradiated, no enhancement of the 2.16 ppm signal was observed, but the base line in this region was more distorted and therefore detection of enhancement would have been even more difficult. [d] Not determined. [e] This is probably a CH_2 on the fatty ester.

cis to each other and endo to the lactone ring (cis/endo), methyls cis to each other and exo to the lactone ring (cis/exo), and the two possible trans orientations of the methyls (transA and transB). These calculations predict the maximum ring pucker for the cyclobutane ring in any of the model structures to be 18° (Table II). This is within the range normally seen for the pucker of substituted cyclobutanes, which rarely exceed 20°, except in cases of severe strain.[18] The maximum dihedral angles for cis substituents of the cyclobutyl ring is 28°. Therefore cis substituents on the cyclobutyl ring will always be closer than trans substituents and the observation of an NOE is an indication that the interacting protons are most likely on the same side of the cyclobutyl ring (cis).

A summary of the NOE results for photoadducts 1 and 3 is shown in Table III. Nomenclature in the following discussions refers to Figure 3. Note particularly the distinction between H-b and CH_2-b and between H-c and CH_2-c. Irradiation of the H-a and CH_3-d signals gave a definite enhancement of the signal from H-b at 2.16 ppm. The NOE interaction of H-b and H-c could not be detected because these signals were too close (2.16 and 2.03 ppm) to allow selective irradiation and observation. It was not possible to accurately detect enhancement of the H-c signal because it was superimposed on other unrelated signals (the α-CH_2 of the fatty acid ester at 2.07 ppm and the CH_3

(18) Fleming, I.; Williams, D. H. *Tetrahedron* **1967**, *23*, 2747–2765.

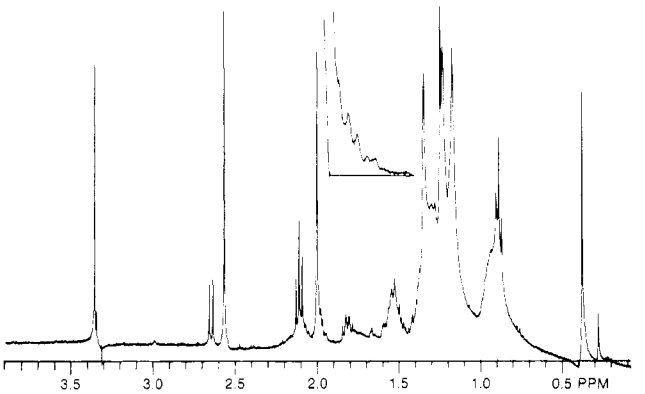

Figure 4. NMR spectrum (400 MHz) of photoadduct 4 from 0 to 3.5 ppm in benzene-d_6. Inset is an enlargement of the region at 2.0 ppm.

at the 5′ position of the furan ring of the furocoumarin at 2.00 ppm). However, separate irradiation of H-b and H-c resulted in definite enhancement of both the H-a and CH_3-d signals. Irradiation of the CH_3-d group at 1.19 or H-c at 2.03 ppm resulted in an NOE response in the signal at 7.01 ppm, which is 5-H on the middle furocoumarin ring. Molecular models indicate that CH_3-d and H-c could be close enough to the furocoumarin 5-H to exhibit NOE interaction. Irradiation of CH_2-b at 1.71 ppm did not lead to enhancement of any of the other cyclobutyl protons; only a signal from the large multiplet at 1.38 representing the fatty acid methylenes was affected. These results indicate that CH_3-d and the three protons at positions a, b, and c are on the same face of the cyclobutane ring.

Results from the NMR analysis of photoadduct 3 were essentially identical with those of photoadduct 1, suggesting that these two adducts have the same stereochemical orientation around the cyclobutane ring. The two protons derived from the OAME double bond have retained the cis orientation. These two protons are on the same face of the cyclobutane ring as the groups derived from the 4-CH_3 and 3-H of the furocoumarin.

Photoadducts 1 and 3 must differ only in the positions of the fatty acid ester and aliphatic side chains with respect to the furocoumarin ring; in one adduct the portion of the fatty acid terminating in the ester group is on position b of the cyclobutane ring (Head-to-Head: HH) and the portion of the fatty acid terminating in the methyl group is on position c; the substitution is reversed in the other adduct (Head-to-Tail: HT). We have not assigned the HH/HT stereochemistry due to difficulty in analyzing the very small differences in the NMR spectra of these two configurations. The adducts have been isolated by using C18 reverse phase HPLC columns that can discriminate subtle differences in the fatty acid moiety. Therefore, differences in the orientation of the fatty acid side chains may significantly affect the chromatographic behavior, but not the ^{1}H NMR spectra.

^{1}H NMR Analysis of Photoadducts 2 and 4. The two photoadducts formed in lower yield, photoadducts 2 and 4, were also isolated, purified, and analyzed by ^{1}H NMR. A portion of the ^{1}H NMR spectrum of photoadduct 2 is shown in Figure 4 and the homonuclear spin-decoupling results are summarized in Table IV. The NMR spectra of these two adducts are essentially identical with each other but differ from the NMR spectra of photoadducts 1 and 3. Several of the substituents on the cyclobutane ring resonate upfield with respect to the same signals in photoadducts 1 and 3. For example, the H-a doublet, at 2.96 ppm in adducts 1 and 3, has shifted upfield to 2.65

Table IV. Results of 400-MHz Decoupling Experiments for Adducts 2 and 4 in Benzene-d_6

chemical shift (ppm)				
adduct 2	adduct 4	mult (integrtn)	coupled[a] to	assignment
7.20	7.20			solvent benzene (residual ^1H)
7.00	7.00	s (1)		[tmPso H-5]
6.08	6.08	s (1)		[tmPso H-4']
3.35	3.35	s (3)		[OAME OCH_3]
2.65	2.65	d (1)	1.98	cyclobutyl H-a [tmPso H-3]
2.59	2.59	s (3)		[tmPso CH_3-8]
2.07	2.07	t (2)		[OAME CH_2-2, α to ester C=O]
2.00	2.00	s (3)		[tmPso CH_3-5']
1.98	1.98	m (2)[b]	2.65[c]	cyclobutyl H-b and H-c [OAME H-9 and 10]
			1.81	
1.81	1.81	q (2)	1.98	cyclobutyl CH_2-b [OAME CH_2-8 or 11]
1.55	1.55	m		[OAME $(CH_2)_n$]
1.42	1.42	m		[OAME $(CH_3)_n$]
1.25	1.25	s (3)		cyclobutyl CH_3-d [tmPso CH_3-4]
1.30–1.08	1.30–1.08	m (overlapping)		[OAME $(CH_2)_n$]
0.97	0.97	t (3)		[OAME 18-CH_3]

[a] See Table I for an explanation of the headings. [b] This integration was uncertain due to overlapping signals. [c] Irradiating at 2.65 ppm caused a change in the shape of one of the signals at 1.98 that could be interpreted as a collapse of a doublet to a signal with other signals superimposed.

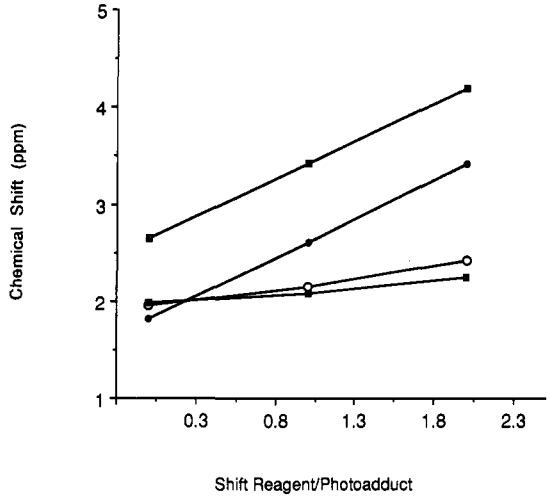

Figure 5. Lanthanide-induced changes in the 400-MHz proton chemical shifts of photoadduct 4. Open squares, H-a; open circles, H-b; closed squares; H-c; closed circles, CH_2-b.

Table V. Results of 500-MHz Homonuclear ^1H NOE Experiments for Photoadduct 2 and 4 in Benzene-d_6

	adduct 2		adduct 4	
irradiated	%NOE	ppm[a]	%NOE	ppm
2.65 ppm cyclobutyl H-a	5.31	1.25 CH_3-d	2.94	1.25 CH_3-d
1.98 ppm cyclobutyl H-b and H-c	none detected[b]		none detected[b]	
1.81 ppm cyclobutyl CH_2-b	5.86	2.65 H-a	5.18	2.65 H-a
	9.01	1.25 CH_3-d	4.06	1.25 CH_3-d
	7.67	1.15 $[(CH_2)_n]$[c]		
1.25 ppm cyclobutyl CH_3-d	3.97	7.01 [H-5 tmPso]	11.28	7.01 [H-5 tmPso]
	4.90	2.65 H-a	11.34	2.65 H-a
	4.08	1.81 CH_2-b	9.38	1.81 CH_2-b

[a] The positions on the cyclobutyl ring are labeled a, b, c, and d as indicated in Figure 3. [b] Interaction of these two protons cannot be detected because they overlap. [c] This is probably a CH_2 on the fatty ester, adjacent to the cyclobutyl CH_2.

ppm in photoadducts 2 and 4.

However, the analysis of adducts 2 and 4 is more difficult than that of adducts 1 and 3 because the resonances of H-b and H-c are superimposed on each other and the furan 5'-CH_3 at 2.00 ppm. Separation of the H-b and H-c resonances at 1.98 ppm was achieved by the addition of a lanthanide shift reagent, Eu(fod)$_3$, to the benzene solution of adduct 4. Incremental additions of Eu(fod)$_3$ led to incremental downfield shifts of the H-a doublet and CH_2-b, the two substituents of the cyclobutane ring that are nearest to the tmPso carbonyl oxygen as shown in Figure 5. Downfield shifts were observed for several other tmPso protons, in proportion to their distance from the carbonyl groups.

Addition of Eu(fod)$_3$ also shifted the H-b and H-c signals downfield. At approximately a 1:1 ratio of Eu(fod)$_3$ to photoadduct, H-b and H-c are still slightly superimposed, with resonances at 2.15 and 2.08 ppm, respectively. They show splitting patterns of a multiplet and a quartet, respectively, similar to that observed for the proton resonances of H-b and H-c at 2.16 and 2.03 ppm in photoadducts 1 and 3. At a 2:1 ratio of Eu(fod)$_3$ to photoadduct, the resonances are shifted further, to 2.24 and 2.42 ppm, respectively, but with significant line broadening that obscures the splitting patterns. These data indicate that the signals at 1.98 ppm in the NMR spectra of photoadducts 2 and 4 can be attributed to that of the coincident resonances of H-b and H-c.

The results of the 500-MHz ^1H NOE experiments for photoadducts 2 and 4 are summarized in Table V. Irradiation of CH_3-d at 1.25 ppm resulted in enhancement of H-a at 2.65 ppm as well as CH_2-b at 1.81 ppm. Irradiation of CH_2-b resulted in the enhancement of H-a and CH_3-d. These results indicate that CH_2-b is on the same face of the cyclobutane ring as H-a and CH_3-d. Therefore H-a and H-b must be trans to each other.

Irradiation of the superimposed signals of H-b and H-c at 1.98 ppm did not result in enhancement of any other resonances. The lack of an NOE signal may be a result of the superimposition of the proton resonances in this region, thereby preventing adequate through-space decoupling of either proton. Although these results suggest that both of these protons are on the opposite face of the cyclobutane ring from the two furocoumarin substituents, the lack of an observable NOE rather may be due to the inadequacy of the NOE experiments in this situation. The NMR signal from the CH_2-c has not been identified, but evidence suggests it is superimposed on the other fatty acid proton resonances and cannot be resolved by the decoupling or NOE experiments.

The coupling constants for the cyclobutyl protons of the four photoadducts are listed in Table VI. These values

Table VI. Coupling Constants of the Cyclobutyl Protons

	adducts 1 and 3 J (Hz)	adducts 2 and 4 J (Hz)
$J_{a,b}$	10.0	8.8
$J_{b,c}$	7.4 ● 0.2	N.D.[a]

[a] Could not be unambiguously determined due to interference from overlapping signals. [b] N.D. = not determined.

were determined from the 2D J-resolved NMR analysis of adduct 1 and the 1D 400-MHz proton spectra of the other adducts. Values reported in the literature for J_{cis} of cyclobutyl rings range from 4.5 to 12 Hz, values for J_{trans} range from 2 to 10.5 Hz, and values for J_{gem} range from −11 to −15 Hz. Generally, J_{cis} is greater than J_{trans} in cyclobutane systems.[19] The coupling constants $J_{a,b}$ of the doublet in photoadducts 1 and 3 is 10 Hz, which is larger than the corresponding coupling constant $J_{a,b}$ of 8.8 Hz in photoadducts 2 and 4. Although the difference between $J_{a,b}$ in the two pairs of photoadducts is small, it is consistent with the NOE results, confirming that H-a and H-b are in the cis orientation in photoadducts 1 and 3 and in the trans orientation in photoadducts 2 and 4.

As for photoadducts 1 and 3, photoadducts 2 and 4 appear to be diastereomers that only differ in the position of the fatty acid side chains on the cyclobutane ring. In these two adducts CH_2-b arising from position 9 or 10 of OAME is on the same face of the cyclobutane ring as the 3-H and 4-CH_3 tmPso substituents. H-b must therefore be on the opposite face of the cyclobutane ring. The position of H-c cannot be determined from the NMR data. Both isomers in which H-b and H-c have retained the cis configuration or the isomers in which isomerization of this bond has occurred to give the trans configuration would fit the NOE results. The configuration of this portion of the structure of adducts 2 and 4 was determined by HPLC analysis described next.

Cis → Trans Isomerization. The quantum yield for cis → trans isomerization of OAME is 0.012, 4 times the sum of the quantum yields for formation of all four adducts, which is 0.003. Within 2 h of irradiation, 6.5% of the total OAME is isomerized to its trans isomer, elaidic acid methyl ester (EAME). The HPLC analyses of the reaction of 4 mM tmPso with 20 mM OAME, with 20 mM EAME, and with 10 mM OAME/10 mM EAME are shown in Figure 6. Note that the retention times for the photoproducts are the same with both fatty acid esters although the relative yields differ. The relative yields of the four adducts in order of their retention times starting with 20 mM OAME are 5:1:5:1, starting with 20 mM EAME are 1:5:1:5, and starting with equal concentrations (10 mM) of OAME and EAME are 1:1:1:1 within experimental uncertainty. The UV spectral properties of the adducts formed from EAME, as determined by the diode array UV absorbance detector, were identical with those of the adducts formed in the OAME irradiation. Since the chromatographic conditions gave greater than base-line resolution of the cis and trans isomers of the parent fatty acid, as well as the two cyclobutane diastereomers differing only by the position of the cis fatty acid alkyl groups, it seems safe to assume that these conditions should also be capable of resolving cyclobutane adducts differing by either the cis or trans orientations of the alkyl side chains. Therefore, these results indicate that photoadducts 2 and 4 are the same as the two major products formed during

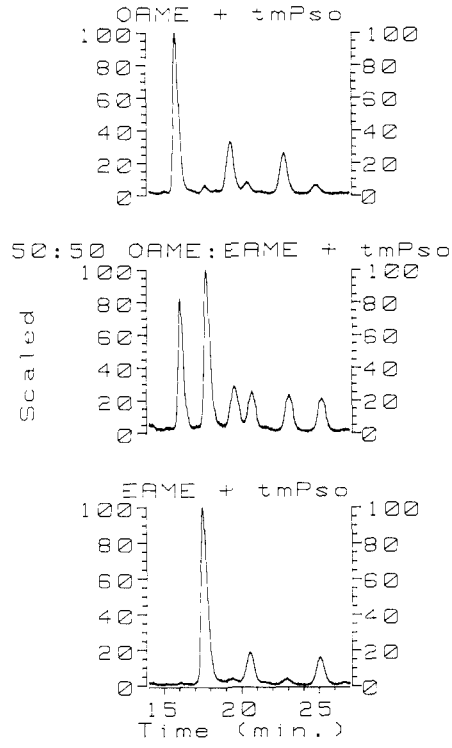

Figure 6. Portion of the HPLC chromatographic analysis of the reaction of 4 mM tmPso with OAME and/or EAME in ethanol, irradiated 1 h. Y-axis = normalized absorbance at 215 nm. Top, 20 mM OAME–4 mM tmPso; middle, 10 mM OAME–10 mM EAME–4 mM tmPso; bottom, 20 mM EAME–4 mM tmPso. Retention times: OAME = 16.0 min; EAME = 18.5 min; photoadducts 1–4 = 19.5, 20.5, 23.0, and 25.0 min., respectively. Chromatographic conditions: Alltech C-18 column (25 × 0.46 cm), 5 μm spherical particles, eluted with 90:10 v/v acetonitrile/water, flow 2.0 mL/min.

the irradiation of EAME, i.e., H-b and H-c are trans in these adducts. Thus the complete configuration of the cyclobutane rings in adducts 2 and 4 are established.

8-MOP Reaction. Four photoadducts were detected by HPLC when 4 mM 8-MOP was illuminated with either 20 mM OAME or EAME. The reaction with 8-MOP was much slower than the same reaction with tmPso for both fatty acids. After 3 h of illumination, HPLC analysis of the solution of 8-MOP and OAME showed four photoadducts formed in nearly equal yields, as measured by peak area. Analysis of the 8-MOP and EAME mixture indicated formation of four photoadducts with identical retention times as those of the OAME–8-MOP adducts, but the yields were in a ratio of 1:9:1:9.

Flash Photolysis. A tmPso excited state triplet intermediate that is quenched by OAME was detected by flash photolysis. The transient decay of 0.096 mM tmPso in oxygen-free ethanol was monitored by the characteristic absorption of the excited triplet at 460 nm. The triplet under these conditions has a first-order decay rate of 2.03×10^5 s^{-1}. When 0.9 mM OAME is added to the tmPso solution, the first-order decay rate of the tmPso triplet increases to 3.26×10^5 s^{-1}. The rate constant for quenching of the tmPso triplet state by OAME was calculated to be $(1.4 \pm 0.5) \times 10^8$ M^{-1} s^{-1}. This represents both chemical and physical quenching of the tmPso triplet by OAME. As a comparison, tmPso quenching by free nucleic acid bases was determined to be 2×10^6 M^{-1} s^{-1} in ethanol.[19]

Solvent Effects. The effect of solvent polarity on the reaction kinetics was determined by irradiating solutions of 20 mM OAME–4 mM tmPso in ethanol, benzene, or cyclohexane for 45 min. At this point less than 50% of

(19) Bensasson, R. V.; Land, E. J.; Truscott, T. G. *Flash Photolysis and Pulse Radiolysis. Contributions to the Chemistry of Biology and Medicine.*; Pergamon Press: New York, 1983; pp 192–208.

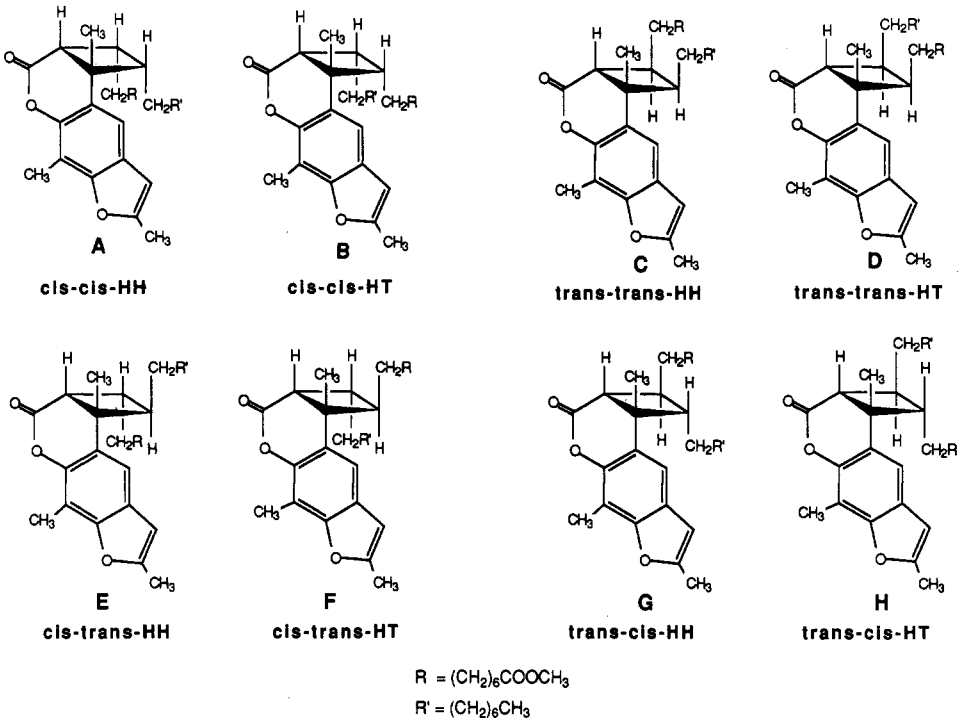

Figure 7. Eight possible diastereomers of OAME–tmPso cyclobutane adducts involving the 3,4-tmPso double bond.

the tmPso is consumed. Solvent polarity strongly affected the reaction rate. Photoadduct yield and cis → trans isomerization (EAME formation) in ethanol were 2.8 times greater than that in benzene and nearly 9.5 times greater than that in cyclohexane. The same product ratios of the four photoadducts and EAME were observed to occur in each solvent system. Intersystem crossing quantum yields of psoralens have been shown to increase by a factor of 3 or more when going from a nonpolar solvent such as benzene to a more polar solvent such as water.[19] Therefore the solvent effect observed also is consistent with the reaction occurring via the tmPso excited triplet state, but the effect of solvent on triplet lifetime, exciplex formation, and diradical formation is not known.

FTIR Analysis. The IR spectra of the four photoadducts in benzene-d_6 solutions are similar. IR absorbances of both the psoralen and fatty acid moieties are observed in the adducts. The cyclobutane ring does not exhibit any particularly characteristic IR spectral features. These results, as well as that for tmPso and OAME, may be found in the supplementary material.

Discussion

Chemical Structures. There are four pairs of diastereomers, illustrated in Figure 7, that could be formed at the 3,4-bond of the furocoumarin. Each of these diastereomers is chiral and can exist in either of two enantiomeric forms, giving a total of 16 stereochemically distinct compounds. The enantiomers were not separated by our HPLC conditions.

Two pairs of diastereomers are possible with the fatty acid retaining the cis configuration at the 9,10-bond. In one pair, H-b is on the same face of the cyclobutane ring as H-a, H-c, and CH_3-d. In the other pair of diastereomers, H-b is on the opposite face of the cyclobutane ring. The members of a pair differ in the position of the fatty acid substituents: one member has the portion of the fatty acid chain with the terminal ester group geminal to H-b and the portion of the fatty acid chain with the terminal methyl group geminal to H-c (Head-to-Head: HH); the other member of the pair has this pattern reversed—the ester terminal group is germinal to H-c and the methyl terminal group is geminal to H-b (Head-to-Tail: HT). A similar set of two pairs of diastereomers could be formed with EAME, the trans isomer of OAME.

The cyclobutane adducts were classified on the basis of the relative orientation of H-a to H-b (cis or trans), the relative orientation of H-c to CH_3-d (cis or trans), and the position of the ester–terminal fatty acid side chain with respect to the coumarin carbonyl group (HH or HT). For example, in the diastereomeric pair A and B in Figure 7, H-a, H-b, and H-c and CH_3-d are all on the same face of the cyclobutane ring. Beginning with the bond closest to the coumarin carbonyl the two diastereomers can therefore be classified as cis-cis-HH and cis-cis-HT, respectively. The other three diastereomer pairs can be classified in the same way. These psoralen–fatty acid adduct geometries are similar to those observed for cyclobutane adducts of psoralen–pyrimidine,[20] except that the fatty acids offer an additional cis–trans configurational option. The nomenclature adopted here is based on the nomenclature most commonly used for cyclobutyl adducts of enones and alkenes in organic chemistry literature rather than the nomenclature most commonly used for psoralens and dipyrimidines.

The NOE experiments indicated that photoadducts 1 and 3, the two adducts formed in highest yield, have similar stereochemical characteristics at the cyclobutane ring. The cis orientation of the fatty acid has been retained and the 9,10 protons are on the same face of the cyclobutane ring as the coumarin proton and methyl group. This is indicative of structures A and B, the all-cis configurations, illustrated in Figure 7. Further classifications based on the orientation of the fatty acid side chains, i.e. HH and HT, were not assigned from the present data because the positions of the fatty acid chains on the cyclobutane ring only have subtle, uninterpretable effects on the ^{1}H NMR spectra.

(20) Baldwin, S. W. *Organic Photochemistry*; Padwa, A. Ed.; Marcel Dekker, Inc.: New York, 1981; Vol. 5, pp 123–225.

The results of the NOE experiments alone indicate that photoadducts 2 and 4 have either the all-trans (C and D) or trans-cis (G and H) stereochemical configurations. The observation of formation of the trans fatty acid ester, EAME, during irradiation of tmPso with OAME suggests that a cyclobutane adduct containing the trans fatty acid is possible. Comparison of the HPLC retention times of tmPso irradiated with OAME, EAME, or 50:50 OAME/EAME solutions indicated that photoadducts 2 and 4 had identical retention times as the two adducts formed in highest yield with EAME. Therefore photoadducts 2 and 4 are established to have trans-cis geometry.

Reaction Mechanism. An abundance of evidence supports the intermediacy of a 1,4-diradical in [2 + 2] photocycloaddition reactions between cyclic enones and alkenes.[20-22] This intermediate usually arises from the triplet excited state of the sensitizer and the ground-state substrate via an exciplex. Starting with a *cis*-alkene, the 1,4-diradical may proceed directly to ring closure, forming cyclobutane adducts with cis stereochemistry. Alternatively, twisting around the 3,4-bond of the olefin in the 1,4-diradical intermediate before ring closure gives cyclobutane adducts with the trans configuration of the alkene substituent. Release of the *trans*-alkene before ring closure is also possible;[22,23] this mechanism of alkene isomerization is named after Schenck. Schenck isomerization involves strong electronic or spin-orbital interaction of the sensitizer and substrate, such as would occur with 1,4-diradical intermediates. This mechanism is often invoked to explain cis → trans isomerization photosensitized by triplets with triplet energies that are too low for direct energy transfer to the alkene (<70 kcal/mol). The tmPso triplet energy is approximately 62 kcal/mol,[19] which implies that Schenck isomerization is more likely than an energy-transfer mechanism for the isomerization of OAME as is observed in the reaction with tmPso.

In this mechanism of cyclobutane formation, the exciplex is probably the species responsible for part of the regioselectivity of the cycloadduct.[20,21] Geometric and steric considerations are important in determining the orientation of the excited triplet and alkene ground state, which then determines the stereochemical structures of the initial bond formed to make the diradical. Structural features of the 1,4-diradicals will determine the efficiency of ring closure, thus determining the product ratios.

All four adducts isolated have a cis configuration between positions c and d of the cyclobutane ring. Two of these adducts also have a cis configuration between positions a and b. Since a trans configuration is not possible between positions a and d due to the constraints imposed by the fused benzofuran ring, the complete stereochemistry of the cyclobutane rings of these adducts is determined by the configuration of bonds a–b and c–d. The trans–cis adducts are formed in lower yield than the cis–cis adducts. No preference is apparent for the HH or HT orientation of the fatty acid side chains.

Initial Bond Formation. We have previously determined[9] that all four adducts are formed with similar kinetics; there is no lag in the production of the trans-cis adducts or free *trans*-EAME compared to the cis-cis adducts. Therefore, the trans fatty ester diradical must be an intermediate on the route to the trans-cis adducts. If it were not, then the formation of the trans-cis adducts, arising from the *trans*-EAME fatty ester that is being formed during the reaction, would lag behind the cis-cis adducts; it would be delayed until significant quantities of the trans fatty ester had accumulated.

Scheme I. Mechanism of the Reaction of OAME with tmPso

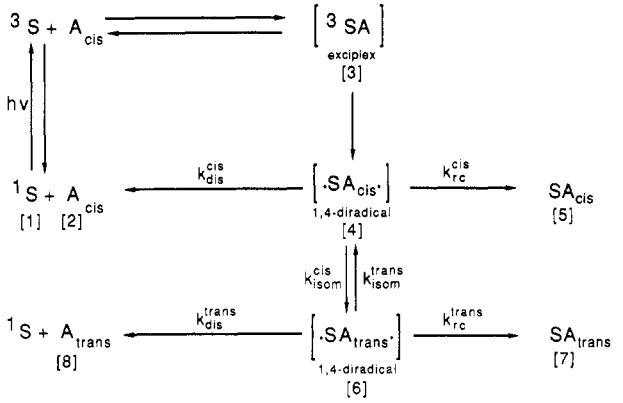

[a] Legend: S = sensitizer (tmPso); A = cis or trans fatty acid; [4] = cis 1,4-diradical; [6] = trans-1,4-diradical; [5] = sum of cis-cis-HH and cis-cis-HT adducts; [7] = sum of trans-cis-HH and trans-cis-HT adducts.

If the trans fatty ester is an intermediate in the formation of the trans-cis adducts, then initial bond formation must occur between positions c and d of the cyclobutane ring, i.e., the tmPso 4-C and one of the OAME olefinic carbons. This conclusion is drawn because no products were detected with a trans geometry at the c–d bond. Selectivity at the point of initial bond formation, perhaps due to the favored geometry of exciplex formation, would account for the lack of formation of adducts with CH_3-d and H-c on opposite sides of the cyclobutyl ring. This selectivity may not be due to steric or electronic effects of the tmPso 4-CH_3 since only four adducts are detected in the reaction of 8-MOP with *cis*-OAME and these adducts have the same HPLC retention time as the adducts formed between 8-MOP and *trans*-EAME. This suggests that there is also selectivity in initial bond formation for 8-MOP, which has a hydrogen at position 4, as with tmPso, which has a methyl at position 4.

Discounting the effect of the 4-CH_3 group in tmPso, there are no steric or electronic effects apparent in models of the ground states of tmPso and OAME that could account for the lack of formation of trans c–d adducts. Therefore, the geometric preference observed for initial bond formation must be due to factors that arise in the excited state of tmPso, the tmPso–OAME exciplex, or the transition state leading to initial bond formation.

Relative Rates of Diradical Reactions. The ratio of cis a–b (adducts 1 + 3) to trans a–b (adducts 2 + 4) adducts is 5:1 when the fatty ester reactant is OAME, indicating less stereoselectivity in ring closure than in initial bond formation. This ratio of cis a–b to trans a–b adducts depends on the relative rates of ring closure, isomerization, and dissociation of the diradical (giving free fatty ester and tmPso). Scheme I illustrates these reaction steps and defines the rate constants for each step. Cis and trans in Scheme I refers to the configuration of the a–b bond. In the following discussion the numbers in brackets refer to the compounds illustrated in Scheme I. [5] corresponds to the sum of adducts 1 + 3, the cis-cis-HH and cis-cis-HT adducts. [7] corresponds to the sum of adducts 2 + 4, the trans-cis-HH and trans-cis-HT adducts. Since the largest amount of EAME formed in the reaction of OAME never exceeds 7% of the OAME and is below 3% until after the

(21) Corey, E. J.; Bass, J. D.; LeMahieu, R.; Mitra, R. B. *J. Am. Chem. Soc.* **1964**, *86*, 5570–5583.
(22) Turro, N. *Modern Molecular Photochemistry*; The Benjamin/Cummings Publishing Co., Inc.: Reading, MA 1978; pp 406–482.
(23) Schenck, G. O.; Steinmetz, R. *Bull. Soc. Chim. Belg.* **1962**, *71*, 781.

reaction is half complete, the rates of the reverse reactions of EAME and the rate of isomerization of the trans diradical are not significant and are therefore neglected. A complete mathematical derivation of the relations used in the following analysis is available as supplementary material.

The quantum yield for *trans*-EAME is 4 times the sum of the quantum yields for all four adducts. [7] is formed at $^1/_5$ the rate of [5], $^1/_6$ the total rate of adduct formation, and therefore $^1/_{24}$ the rate of EAME. Thus the rate of dissociation of the trans diradical [6] is 24 times faster than the rate of ring closure of this intermediate, since these rate constants alone determine the ratio of EAME to trans a–b adducts. assuming that the concentration of [6] is relatively constant during the reaction (steady state), then the rate of isomerization of the cis diradical [4] is 5 times faster than its rate of ring closure, as determined from the rate of dissociation of [6] and the relative yields of the [5] to [7] (5:1).

A similar analysis can be performed for the reaction starting with 20 mM EAME and no OAME. In this case, the reactions of OAME and the isomerization of the cis diradical are insignificant and are neglected. The yield of OAME in this reaction was too low to measure accurately, but based on the detection limit for OAME it is concluded that the rate of dissociation of the cis diradical is slower than or equal to the rate of ring closure of the cis diradical and the rate of ring closure of the trans diradical is 2.5 to 5 times faster than isomerization.

The rates of any of the reactions of the cis diradical relative to any of the reactions of the trans diradical cannot be determined from the available data, since the relative concentrations of the diradicals (or their relative rates of formation) are not known. The most that can be said is that any difference in rates of formation of the diradicals is compensated by differences in the rates of ring closure, since the rates of formation of the cis and trans adducts are equal when the initial concentrations of the cis and trans fatty ester are equal.

Conclusions

When OAME and tmPso are irradiated with 360-nm UV light, four cyclobutane-linked covalent adducts are formed. Two of these adducts have a cis-cis configuration about the cyclobutane ring and two have a trans-cis configuration. The lack of formation of the cis-trans and trans-trans adducts may be due to the geometry of exciplex formation.

The site of initial bond formation was established to be the 4 position of tmPso with either the 9 or 10 position of the fatty ester. This reaction most likely results in the formation of a diradical intermediate. The relative rates of dissociation and ring closure for the cis diradical are comparable whereas the relative rate of dissociation is 24 times greater than the rate of ring closure for the trans diradical. The rate of cis → trans isomerization of the 9,10-bond of the fatty ester portion of the diradial is about 5 times the rate of ring closure for the cis diradical but only about $^1/_5$ the rate of ring closure for the trans diradical.

Experimental Section

Chemicals. 4,5′,8-Trimethylpsoralen (tmPso) and 8-methoxypsoralen (8-MOP) were obtained commercially (Aldrich Chemical Co., Milwaukee, WI) and used without further purification. Oleic and elaidic acid methyl esters were obtained from Sigma Chemical Co (St. Louis, MO). DMC (4,8-dimethyl-7-methoxycoumarin) and DAC (4,8-dimethyl-7-acetoxycoumarin) were a gift from Dr. Heindel, Lehigh University, Bethlehem, PA. Solvents were spectrophotometrically pure HPLC grade. NMR samples were dissolved in benzene-d_6 (100.0 atom % D) obtained from Aldrich Chemical Co. The lanthanide shift reagent, Resolve-Al EuFOD, europium (1,1,1,2,2,3,3-heptafluoro-7,7-dimethyl-4,6-octanedionate), was also obtained from Aldrich Chemical Company and vacuum desiccated before use.

Irradiation and Isolation Procedures. Solutions of 4 mM tmPso and 20 mM OAME were illuminated, with stirring, at 15 ± 2 °C. The samples were irradiated 2 cm from the light source, with a bank of four General Electric F15T8 BLB fluorescent lamps having maximum emission centered at 360 nm. The light flux at the surface of the samples was 25 $J\ m^{-2}\ s^{-1}$ as determined by potassium ferrioxalate actinometry.[24]

The reaction mixtures were analyzed by C-18 reverse phase HPLC using an Alltech analytical C-18 column, 250 × 4.6 mm, 5-μm spherical particles (Alltech Associates, Deerfield, IL), and eluting with CH_3CN/H_2O, 90:10 (v/v), at a flow rate of 2.0 mL/min. The absorbance of the eluent was monitored by using a Hewlett-Packard Model 1090 diode array detector (Hewlett-Packard, Co., Palo Alto, CA).

Photoproducts were isolated by irradiating 20 mM OAME and 4 mM tmPso in ethanol for 2–4 h in 50-mL glass test tubes with screw caps. The samples were concentrated by rotary evaporation at <40 °C and then fractionated by using a Harrison Research Model 7924 chromatotron spinning disk TLC apparatus with a 2-mm silica gel 60F spinning disk purchased from Analtech (Newark, DE) and eluting with hexane/ethyl acetate (19:1 v/v). Bands were detected by 254-nm fluorescence blocking. The second band, which contained the four OAME–tmPso photoproducts, was collected, concentrated, and injected into a Nucleosil C-18 preparative HPLC column, 10 mm × 50 cm, 7-μm particles (Alltech Associates, Deerfield, IL) and eluted with acetonitrile/water (85:15 v/v) at a flow rate of 5.0 mL/min. Each of the photoproducts was then lyophilized and repurified by preparative HPLC. The isolated photoproducts were stored at −40 °C, in the dark, under nitrogen or argon.

Quantum Yield Measurements. Two-milliliter samples were irradiated in 2-mL screwcap vials, with stirring, as described above. Quantum yields for adduct formation were calculated by using ^{3}H-labeled tmPso. The HPLC peaks corresponding to adducts were collected in scintillation vials after measured periods of illumination, the solvent was evaporated with a stream of air at 37 °C, and the residue was redissolved in 150 μL of ethanol and 10 mL of a dioxane based scintillation cocktail (120 g of naphthalene, 4 g of PPO, 0.05 g of POPOP/L dioxane). The radioactivity was measured with a Beckman LS-7500 liquid scintillation counter in the single channel mode correcting for quenching and efficiency. The molar specific activity of the adducts was assumed to be the same as that of the tmPso reactant.

The incident light intensity was determined under the same conditions by irradiating 2 mL of an aqueous 0.006 M ferrioxalate actinometer solution[24] in the same type of vials, with stirring. Under these conditions the concentrations of tmPso and ferrioxalate are sufficiently high so that all of the incident light is absorbed. The difference between the indices of refraction of the two solvents is within the experimental error, and the sample vials are identical, so this method should give a fairly accurate measurement of the amount of light absorbed by the reaction solution. The BLB blacklights have an emission band from 300 to 400 nm with maximal emision at 360 nm. The incident light on the solution was determined to be $(2.1 \pm 0.1) \times 10^{-6}$ E/min.

The quantum yield of EAME formation was determined under identical irradiation conditions. The concentration of EAME was determined from the area of the peak corresponding to EAME by using a calibration curve of EAME concentration versus peak area measured from the HPLC chromatograms of standard solutions of EAME injected under identical chromatographic conditions.

^{1}H NMR Analysis. After purification the solvent was removed by rotary evaporation at <40 °C and the photoproducts were redissolved in benzene-d_6. One-dimensional ^{1}H NMR spectra were obtained on a Varian XL-400 spectrometer. An 8K data set covering a 1300-Hz spectral window resulted in 0.32 Hz/pt digital resolution; 128 transients were accumulated before Fourier

(24) Calvert, J. G.; Pitts, J. N., Jr. In *Photochemistry*; Wiley: New York, 1966; pp 783–787. Hatchard, C. G., Parker, C. A. *Proc. R. Soc.* **1956**, *A235*, 518–536.

transformation and 1-Hz line broadening was applied.

Two-dimensional COSY and J-resolved NMR spectra were obtained on a Bruker WM-300 spectrometer. 2K × 2K data points cover 2400 × 2400 Hz resulting in about 2.4 Hz/pt digital resolution. Data was collected for 256 T_1 values and then zero-filled to 1K; 96 scans were accumulated for each T_1.

The NOE experiments were conducted on a Bruker WM-500 NMR spectrometer. Peak irradiation was conducted at a power level below saturation of the signal in an 8-s time period and was followed after a 15 ms delay by a 90° observe pulse and 3 s of data acquisition with an additional 1-s delay between cycles. Sixteen transients were collected per multiplet irradiated. On-resonance transients were interleaved with off-resonance transients. The 32K point FID of the off resonance control experiment was subtracted from that of the on resonance experiment and Fourier transformed with 0.5-Hz line broadening.

High Resolution Mass Spectrometry. High resolution electron impact mass spectra were obtained with a VG 79S mass spectrometer using a DCI probe, 70 eV electron energy and 180 °C source block, 10^{-8} accuracy, 0.3-s response time, 100-μA trap current, and 6.6K/1000 resolution.

FTIR Analysis. IR spectra were acquired on a Nicolet Fourier transform IR Model 20DX spectrophotometer containing a IIIb HeNe laser with 4.0 cm^{-1} resolution. The photoadducts were dissolved in benzene-d_6 and placed in sodium chloride cells with 0.015-mm spacers. Interference from benzene-d_6 absorbance was minimized by spectral subtraction after Fourier transformation.

Flash Photolysis Experiments. Flash photolysis experiments were performed with the help of Dr. T. George Truscott at the Department of Chemistry, Paisley College of Technology, Scotland. The experimental system used the frequency doubled (347 nm) output from a J. K. Laser Ruby laser with data analysis using a digitiser/Apple computer system. Samples were dissolved in ethanol and bubbled with oxygen-free argon or nitrogen prior to measurements.

Molecular Mechanics Calculations. Molecular mechanics energy minimization calculations were performed by using Allinger's MM2 program available as program no. 395 from QCPE, Department of Chemistry, Indiana University, Bloomington, IN. A fragment of the tmPso–OAME adducts containing the cyclobutane ring fused to the six-membered lactone ring portion of tmPso, including the 4-CH_3 group was used. The benzofuran ring that is fused to the lactone ring in the furocoumarin was not included to simplify calculations. This benzofuran ring would be expected to decrease the pucker of the cyclobutyl ring due to the constraint it would impose on the flexibility of the lactone ring and therefore the absence of the benzofuran ring should lead to an overestimation of the ring pucker. Calculations were performed for the molecules with methyl groups representing the fatty acid chains in all four of the possible configurations. The presence of methyl groups instead of long alkyl chains should not dramatically alter the results in terms of the pucker of the cyclobutyl ring. To check this assumption, we also performed calculations with the same molecules with hydrogens in place of the methyl groups. The results of these calculations showed that the methyl group caused the ring to flatten relative to the H-substituted analogues (data not shown) and, therefore, the larger alkyl substituents of the fatty acids at these positions would not be expected to cause a large increase in cyclobutyl ring pucker relative to the methyl-substituted models.

Acknowledgment. We thank Prof. George Truscott, Department of Chemistry, Paisley College of Technology, Scotland, for his valuable assistance in the flash photolysis studies of psoralen triplet quenching by OAME and the use of his equipment. We are also grateful to Prof. George Clemans of the Department of Chemistry, Bowling Green State University, for performing the molecular mechanics calculations and expert advice. We acknowledge the use of the following facilities: high resolution EI mass spectra obtained by Dr. Joseph L. Kachinski, Jr. in the Department of Chemistry, Johns Hopkins University, Baltimore, MD; 300-MHz 2D COSY and J-resolved ^{1}H NMR spectra obtained at the Johns Hopkins University Biophysics NMR Facility established by NIH grant GM27512 guided by Facility Coordinator, Prof. Lou-Sing Kan; 400-MHz ^{1}H NMR spectra obtained at the Johns Hopkins Chemistry Department NMR Facility established by NIH grant SIO RR01934 and NSF grant PCM 83-03176, and 500-MHz ^{1}H NOE NMR experiments performed at the Chemical Instrument Center of the Ohio State University Chemistry Department in Columbus, OH, expertly assisted and advised by Center Director, Dr. Chuck Cottrell. We are grateful for financial support from NIH grants ES03841 and ES02300. This is publication 49 from the Center for Photochemical Sciences, Bowling Green State University.

Supplementary Material Available: More details on the ^{1}H NMR assignments of trimethylpsoralen and the coumarin model compounds, the FTIR results, and the kinetic derivation and analysis (6 pages). Ordering information is given on any current masthead page.

Iminium Ion Mediated Cyclizations of 4-Aryl-1,4-dihydropyridines. Regio- and Stereoselective Intermolecular Cycloaddition Reactions

George D. Hartman,* Brian T. Phillips, Wasyl Halczenko, and Steven M. Pitzenberger

Merck Sharp & Dohme Research Laboratories, West Point, Pennsylvania 19486

Received March 8, 1989

Cyclopentadiene and furan undergo efficient regio- and stereoselective intermolecular inverse electron demand cycloaddition to the dihydropyridine iminium ion under Lewis acid conditions. However, the reaction is quite sensitive to both steric and electronic factors in the nucleophilic component. Synthetically useful cyclization is restricted to unhindered styrenes, cyclopentadiene, and reactive aromatic compounds such as furan. The initial example of an intermolecular cycloaddition in this series involving a thioether is described.

We and others have reported a variety of novel intramolecular cycloaddition processes of appropriately substituted 4-aryl-1,4-dihydropyridines.[1] Similar imminium ion mediated processes have been shown by Wenkert,[2]

0022-3263/89/1954-4134$01.50/0